High Aspect Ratio Nanomaterials Enable Biomolecule Delivery and Transgene Expression or Silencing in Mature Plants

Gozde S. Demirer[1], Huan Zhang[1], Juliana L. Matos[2,3], Roger Chang[1], Linda Chio[1], Brian Staskawicz[2,3] and Markita P. Landry[1,4,5]*

[1] Department of Chemical and Biomolecular Engineering, University of California, Berkeley, CA 94720, USA.
[2] Department of Plant and Microbial Biology, University of California, Berkeley, CA 94720, USA.
[3] Innovative Genomics Institute (IGI), Berkeley, CA 94720, USA.
[4] California Institute for Quantitative Biosciences, QB3, University of California, Berkeley, CA 94720, USA.
[5] Chan-Zuckerberg Biohub, San Francisco, CA 94158, USA.
*e-mail: landry@berkeley.edu

Genetic engineering of plants is at the core of sustainability efforts, natural product synthesis, and agricultural crop engineering. The plant cell wall is often a barrier that limits the ease and throughput with which exogenous biomolecules can be delivered to plants. Current delivery techniques suffer from host range limitations, low transformation efficiencies, toxicity, and unavoidable DNA integration into the host genome. Here, we demonstrate efficient diffusion-based biomolecule delivery into several species of mature plants with a suite of pristine and chemically-functionalized high aspect ratio nanomaterials. Efficient DNA delivery and strong transient protein expression is accomplished in mature *Eruca sativa* (arugula-dicot) and *Triticum aestivum* (wheat-monocot) leaves and protoplasts. We also demonstrate a second nanoparticle-based strategy in which small interfering RNA (siRNA) is delivered to mature *Nicotiana benthamiana* leaves, to effectively silence a gene with 95% efficiency. Our work provides a tool for species-independent, targeted, and passive delivery of genetic material, without transgene integration, into plant cells for diverse plant biotechnology applications.

Plant biotechnology is critical to address the world's leading challenges in meeting our growing food and energy demands, and as a tool for scalable pharmaceutical manufacturing. Over the past several decades, remarkable progress has been made in biotechnology with the improvement of genome editing and sequencing tools. Owing to these recent advancements, plant synthetic biology and bioengineering now has tremendous potential to benefit many fields. In agriculture, genetic enhancement of plants can be employed to create crops that are resistant to herbicides[1], insects[2], diseases[3], and drought.[4] In pharmaceuticals and therapeutics, genetically engineered plants can be used to synthesize valuable small-molecule drugs and recombinant proteins[5]. Furthermore, bioengineered plants may provide cleaner and more efficient biofuels[6,7].

Despite several decades of advancements in biotechnology, most plant species remain difficult to genetically transform[8]. One of the major challenges facing efficient plant genetic transformation is biomolecule delivery into plant cells through the rigid and multi-layered cell wall. Currently, few delivery tools exist that can transfer biomolecules into plant cells, each with considerable limitations. Agrobacterium-mediated delivery[9] is the most commonly used tool for gene delivery into plants with limitations of efficient delivery to only a narrow range of plant species, inability to perform DNA-free editing, unsuitability for high-throughput applications, and unavoidable DNA integration into the plant host genome[10]. The one other commonly used tool for plant transformation is biolistic particle delivery (also called gene gun)[11], which can deliver biomolecules into a wider range of plant species but faces limitations of low-level and sporadic expression, potential toxicity of the particles used[12], and plant tissue damage from high bombardment pressures[8]. Therefore, for plant engineering to reach its full potential, conventional gene delivery methods are due for significant modernization commensurate with advances in molecular biotechnology to address aforementioned limitations.

Nanomaterials are optimal candidates to eliminate current limitations of biomolecule delivery into plants. While nanomaterials have been studied for gene delivery into animal cells[13,14], their potential for plant systems remains under-studied[15]. Under certain surface chemistries, high aspect ratio nanomaterials such as carbon nanotubes (CNTs) have recently been shown to traverse extracted chloroplast[16] and plant[17] membranes with several figures of merit: high aspect ratio, exceptional tensile strength, high surface area-to-volume ratio, and good biocompatibility. When bound to CNTs, biomolecules are protected from cellular metabolism and degradation[18], exhibiting superior biostability compared to free biomolecules. Moreover, single-walled carbon nanotubes (SWCNTs) have strong intrinsic near-infrared fluorescence[19,20] within

the tissue-transparency window and thus benefit from reduced photon scattering, allowing for tracking of cargo-nanoparticle complexes deep in plant tissues. However, previous incorporation of CNTs in plant systems is limited to exploratory studies of CNT biocompatibility[16,21,22] and sensing of small molecules in plant tissues[17,23] by introducing CNTs complexed to fluorescent dyes or polymers with no biological function.

Herein, we develop a CNT-based platform that can deliver functional biomolecules into both model and crop plants with high efficiency. We used covalently-functionalized or pristine CNTs to deliver DNA into mature arugula (dicot) and wheat (monocot) leaves, and obtained strong transient protein expression, with efficiencies comparable to *Agrobacterium*-mediated and higher than biolistic particle delivery. We also show nanotube-based transient protein expression in arugula protoplasts with 85% transformation efficiency. Lastly, we achieve 95% gene silencing in *Nicotiana benthamiana* leaves through CNT mediated delivery of siRNA. This study establishes efficient transient gene expression and silencing in mature plants, for the first time, through passive CNT-mediated delivery of functional biomolecules and can enable high-throughput genetic plant transformations for a variety of plant biotechnology applications.

RESULTS

In this work, expression of a functional gene is accomplished by delivering plasmids and linear DNA fragments into the mature plant cell nucleus with CNTs, in arugula and wheat true leaves, and in arugula protoplasts. Separately, alternate grafting chemistries enable gene silencing in mature *Nicotiana benthamiana* true leaves, achieved by delivering siRNA into the plant cell cytoplasm with CNT-based nanocarriers (**Fig. 1a**). Additionally, different CNT formulations are tested for efficiency optimization, and the transient nature of CNT-mediated expression and silencing is demonstrated by quantifying the mRNA transcript and functional protein levels.

Grafting DNA on carbon nanotube scaffolds

For the transgene expression study, we developed two distinct grafting methods to load green fluorescent protein (GFP)-encoding plasmids or their linear PCR fragments on SWCNTs and multi-walled carbon nanotubes (MWCNTs). The first DNA-grafting method involves direct adsorption of DNA on CNTs via dialysis. Initially, CNTs are coated with a surfactant – sodium dodecyl sulfate (SDS). During dialysis, SDS desorbs from the CNT surface and exits the dialysis membrane, while DNA adsorbs onto the surface of CNTs in a dynamic ligand exchange process (**Fig. 1b**). In this method, double-stranded DNA vectors graft on CNTs through π-π stacking

interactions. The adsorption of DNA on CNTs is confirmed through a solvatochromic shift in the SWCNT near-infrared fluorescence emission spectra; characteristic of a DNA adsorption-induced change in the CNT dielectric environment[24] (**Supplementary Fig. 1**). Control dialysis aliquots of SDS coated CNTs, in the absence of DNA, show rapid CNT precipitation and lack near-infrared fluorescence (**Supplementary Fig. 1**), confirming SDS desorption and replacement by DNA in our dialysis aliquots with DNA. Stable adsorption of DNA on CNTs is separately confirmed via agarose gel electrophoresis (**Supplementary Fig. 1**). Additionally, at the end of the dialysis procedure, we confirmed that there is no SDS left in the cartridge, by using Stains-all dye (see Methods and **Supplementary Fig. 1**).

The second method developed for DNA grafting on CNTs is electrostatic grafting, in which carboxylated CNTs (COOH-CNT) are first covalently modified with a cationic polymer (poly-ethyleneimine, PEI) to carry a net positive charge. Next, positively charged CNTs (PEI-CNT) are incubated with negatively charged DNA vectors (**Fig. 1c**). The covalent attachment of PEI and electrostatic adsorption of DNA on CNTs is confirmed through zeta potential measurements (**Fig. 1d**), after extensive washing of free unreacted PEI (see Methods). The initial zeta potential of -24.1 mV for COOH-CNT increases to +47.4 mV after reaction with positively-charged PEI, and subsequently decreases to +31.7 mV when incubated with negatively charged DNA, confirming DNA adsorption. Additionally, atomic force microscopy (AFM) imaging of nanoparticles confirms CNT functionalization and DNA adsorption to CNTs via CNT height increases (**Fig. 1e** and **Supplementary Fig. 2**). Nanoparticle heights before and after reaction with PEI are measured to be 6.0 nm and 12.1 nm for COOH- and PEI-MWCNT, respectively, confirming PEI binding. AFM also reveals that CNT height increases from 12.1 nm to 22.8 nm after incubation with DNA vectors, as expected, further confirming DNA grafting on CNTs.

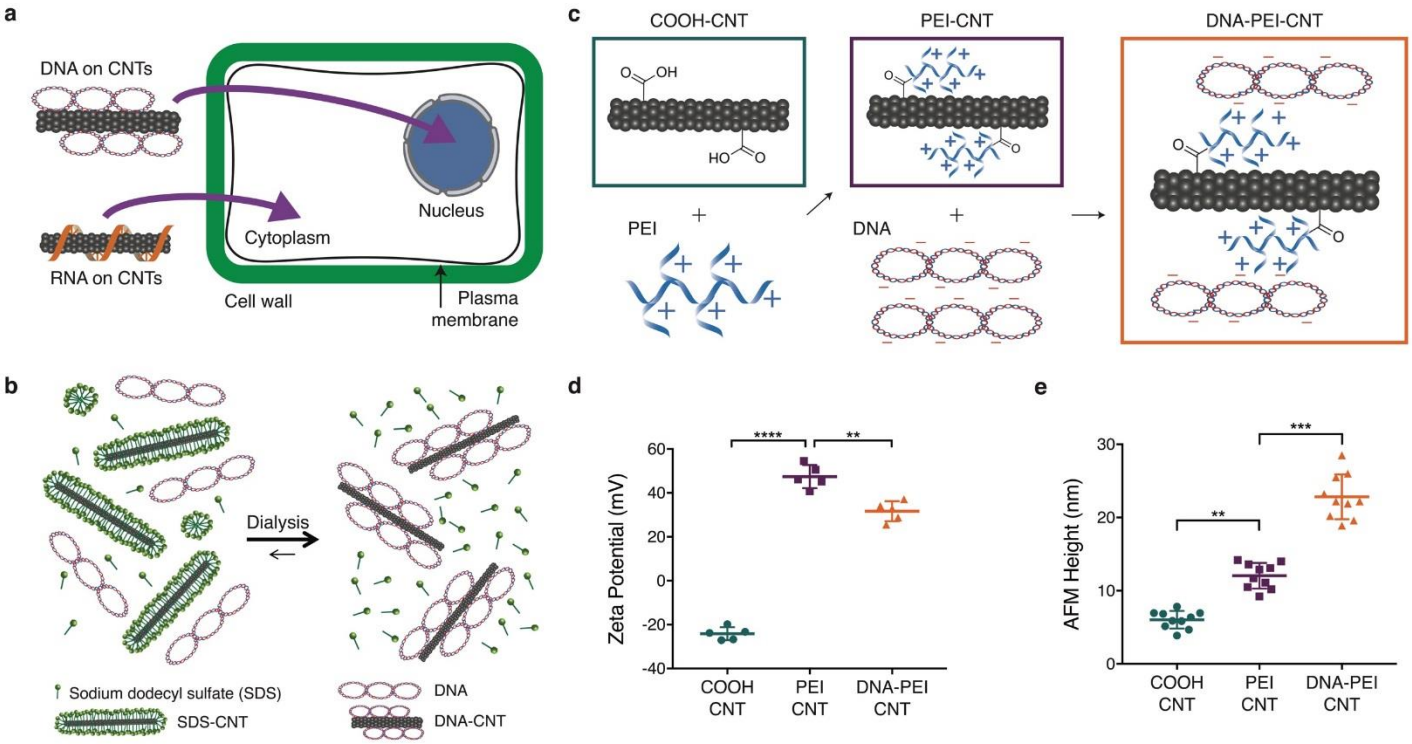

Figure 1. Overarching strategy for CNT-mediated plant transformations and DNA grafting on CNTs (**a**) For expression of a functional gene, DNA is delivered into the mature plant cell nucleus with carbon nanotubes. Separately, for silencing of a functional gene, siRNA is delivered into the plant cell cytoplasm with carbon nanotubes. (**b**) DNA is grafted on CNTs through π-π stacking, in which the initial SDS coating is gradually replaced by DNA adsorption through dialysis. (**c**) Carboxylated CNTs (COOH-CNT) are first chemically modified via covalent attachment of a cationic PEI polymer (PEI-CNT), and subsequently incubated with negatively charged DNA to form DNA loaded PEI-CNTs (DNA-PEI-CNT). (**d**) PEI and DNA binding on CNTs is validated by zeta potential measurements: The -24.1 mV zeta potential of COOH-CNT increases to +47.4 mV after reaction with PEI, due to positively charged PEI binding, and subsequently decreases to +31.7 mV when incubated with negatively charged DNA, confirming DNA adsorption. ***P* = 0.0086 and *****P* < 0.0001 in one-way ANOVA. Error bars indicate s.d. (n = 5). (**e**) Average height profile of CNTs is obtained through AFM imaging. Nanoparticle heights before and after reaction with PEI are measured to be 6.0 and 12.1 nm for COOH- and PEI-CNT, respectively, confirming PEI binding. CNT nanoparticle height increases from 12.1 to 22.8 nm after incubation with DNA vectors, confirming DNA grafting. ***P* = 0.02 and ****P* = 0.0002 in one-way ANOVA. Error bars indicate s.d. (n = 10).

DNA delivery into mature plants with carbon nanotube scaffolds

Functional gene expression studies are implemented with arugula (*Eruca sativa*) to demonstrate the applicability of our platform to transform crop plants in lieu of traditional laboratory plant species. Furthermore, the expression studies are carried out with wheat (*Triticum aestivum*) plants, which are monocots that cannot be efficiently transformed in a genotype independent manner through *Agrobacterium*-mediated delivery.

After GFP-encoding DNA-CNT suspensions are prepared through dialysis or electrostatic grafting, they are infiltrated into the true leaves of mature arugula and wheat plants (see

Methods). Post-infiltration, DNA-CNTs traverse the plant cell wall and membrane to enter the cytosol. In the cytosol, we postulate that either the DNA-CNT complex further transports across the nuclear membrane where DNA desorbs from the CNT surface, or DNA desorbs from the CNT surface inside the cytosol and free DNA travels into the nucleus to initiate gene expression (**Fig. 2a**). Leaves infiltrated with DNA-CNTs are imaged with confocal microscopy, and expression of GFP is observed in the cells of the leaf lamina 72-hours post-infiltration both in arugula and wheat plants (**Fig. 2b**). Z-stack analysis of the fluorescence profile of the DNA-CNT treated leaves shows that GFP fluorescence originates from the full thickness of the leaves, confirming that CNT nanocarriers diffuse and penetrate through the full leaf profile by percolating through ~5 layers of plant cells (**Fig. 2c**). No GFP expression is detected in the leaves when free DNA vectors, PEI-DNA complexes, or PEI-CNTs are delivered in control studies (**Supplementary Fig. 3**).

The efficiency of CNT nanocarrier internalization and GFP expression varies widely for the different nanomaterial formulations we tested. Quantitative fluorescence intensity analysis of confocal images for arugula leaves (see Methods) indicates that GFP expression is significantly higher for DNA-CNTs prepared through electrostatic grafting compared to GFP expression induced by DNA-CNT conjugates prepared via dialysis (**Fig. 2d**). Our most efficient DNA-CNT formulation is plasmid DNA delivered with PEI-functionalized SWCNT, which is over 700 times more efficient than plasmid DNA adsorbed on pristine MWCNT via dialysis, our least-efficient DNA-CNT formulation. Our results suggest that the CNT surface chemistry is an important factor for biomolecule delivery into plant cells. The observed results can be explained by different DNA binding affinities to CNT surfaces in the two DNA grafting methods. The predominant DNA-CNT binding interaction in the case of dialysis is π-π stacking. In contrast, electrostatic attraction is the predominant binding interaction for the electrostatic grafting method. We propose that the smaller equilibrium dissociation constant[25] and higher binding energy value[26,27] for electrostatic attraction compared to π-π stacking interactions increase the stability of the DNA-CNT complex as it traverses the cell wall, plasma membrane, and nuclear envelope, thus increasing the delivery efficiency of DNA to the plant cell nucleus.

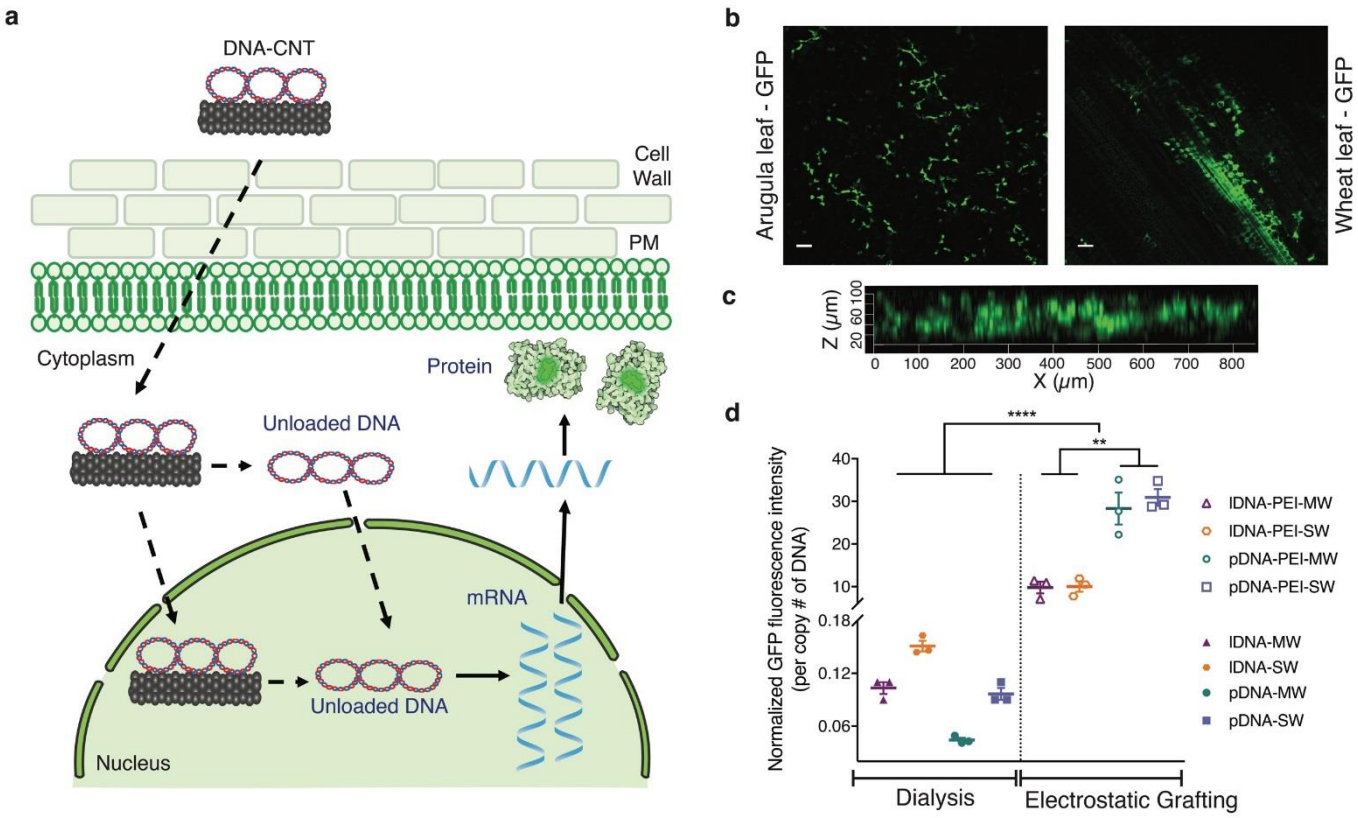

Figure 2. DNA delivery into mature plants with CNTs and subsequent GFP expression. (**a**) DNA-CNTs traverse the plant cell wall and membrane and enter the cytosol where DNA either desorbs in the cytosol and enters the nucleus, or DNA carried by CNTs is transported across the nuclear membrane to initiate gene expression. Dotted lines represent trafficking steps and the rigid lines represent gene expression steps. (**b**) Arugula (dicot) and wheat (monocot) leaves infiltrated with DNA-CNTs are imaged with confocal microscopy, and expression of GFP is observed in the leaf lamina. Scale bars, 50 μm. (**c**) Z-stack analysis of the fluorescence profile of the DNA-CNT treated arugula leaf shows that GFP fluorescence originates from the full thickness of the leaf, confirming that CNT nanocarriers diffuse and penetrate through the full leaf profile. (**d**) Quantitative fluorescence intensity analysis of arugula confocal images indicates that GFP expression is significantly higher for DNA-CNTs prepared by electrostatic grafting compared to GFP expression induced by DNA-CNTs prepared via dialysis. $^{**}P = 0.001$ and $^{****}P < 0.0001$ in one-way ANOVA. Error bars indicate s.e.m. (n = 3).

Independent of the nanomaterial formulation or plant species, we further demonstrate that CNT-mediated gene expression is transient in mature plant leaves. Representative confocal images of DNA-CNT infiltrated arugula and wheat leaves (**Fig. 3a**) and corresponding quantitative fluorescence intensity analysis of these images demonstrate that the highest GFP fluorescence intensity at Day 3 disappears by Day 10 (**Fig. 3b**). Similarly, quantitative PCR (qPCR) analysis of GFP mRNA collaborates our confocal imaging results. For DNA-CNT treated arugula leaves, we observe an over 7500-fold GFP mRNA change 3-days post-infiltration, which drops to an insignificant two-fold mRNA change by Day 10 in DNA-CNT treated arugula leaves, as compared to non-treated arugula leaves (**Fig. 3c**). Our results both at the mRNA transcript and fluorescent protein expression levels demonstrate that GFP expression is transient and

suggest that genes delivered into plant cells via CNT carriers do not integrate into the plant nuclear genome. Compared to CNT-mediated expression, however, *Agrobacterium*-mediated GFP expression in mature arugula leaves (see Methods) did not cease at Day 10 (**Supplementary Fig. 4**), supporting the established concept of DNA integration in the case of *Agrobacterium*-mediated delivery [28].

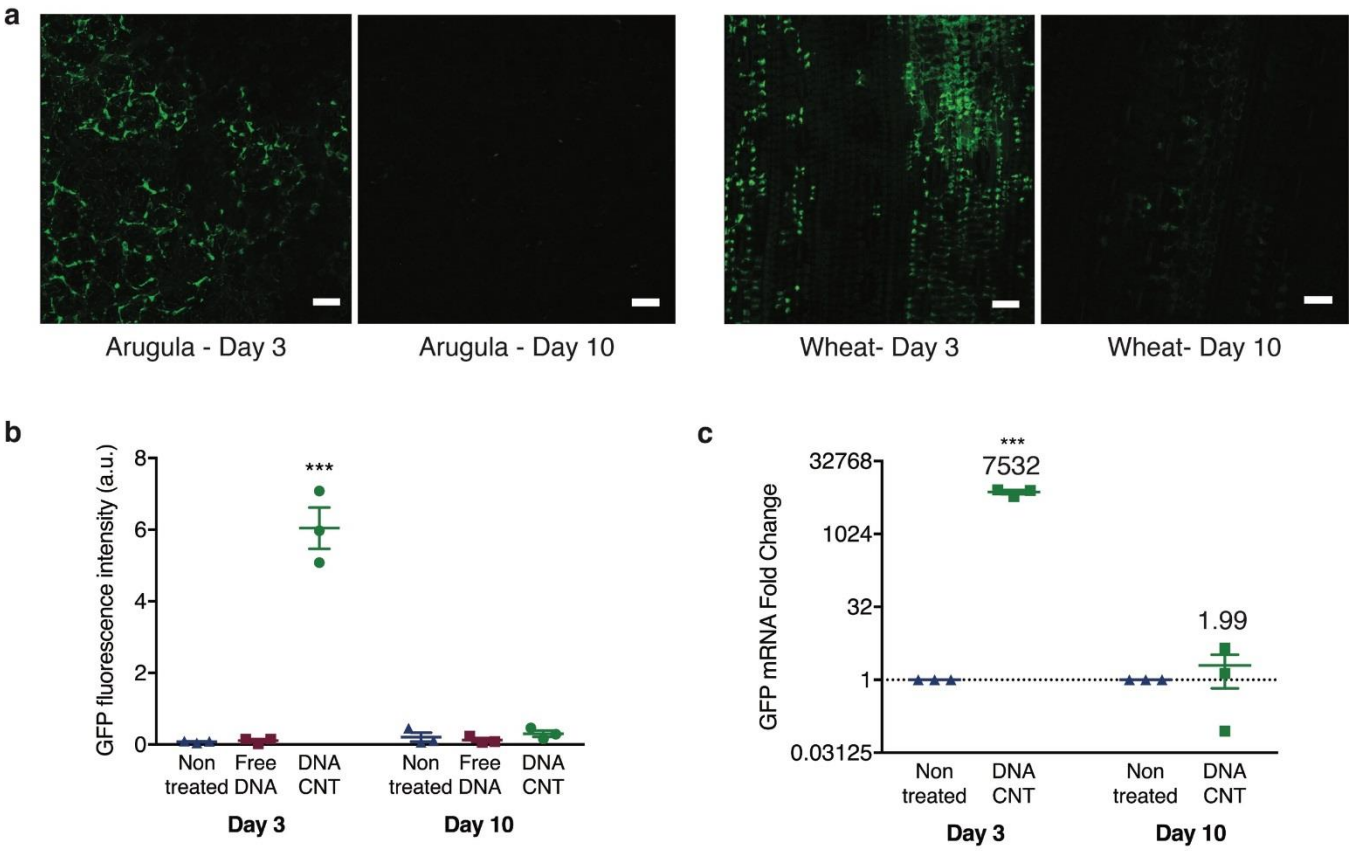

Figure 3. CNT-mediated GFP expression is transient in arugula and wheat leaves. (**a**) Representative confocal microscopy images showing GFP expression at Day 3 and no to minimal expression at Day 10 in DNA-CNT infiltrated mature arugula and wheat leaves. Scale bars, 50 µm (**b**) Quantitative fluorescence intensity analysis of confocal images demonstrating that GFP expression at Day 3 induced by CNT-mediated DNA delivery disappears 10-days post-infiltration. ****P* = 0.0001 in two-way ANOVA. Error bars indicate s.e.m. (n = 3). (**c**) Quantitative PCR analysis show over 7500-fold GFP mRNA change at Day 3, dropping to a 2-fold change at Day 10 in DNA-CNT treated arugula leaves compared to the non-treated leaves. ****P* = 0.0003 in two-way ANOVA. Error bars indicate s.e.m. (n = 3).

Biolistic (gene gun-based) DNA delivery is a leading technique for transformation of plant species that are incompatible with *Agrobacterium*-based transformation. We next compared CNT-mediated DNA delivery with biolistic particle DNA delivery by transforming mature arugula true leaves and cotyledons with the same GFP-encoding plasmid using a gene gun (see Methods). Interestingly, we did not obtain GFP expression in arugula true leaves, and observed

sparse GFP expression only in the guard cells of arugula cotyledons through biolistic delivery (**Supplementary Fig. 4**). Since GFP expression is limited to the topmost layer of the cotyledons, it is likely that the gene gun DNA delivery method cannot penetrate deep enough in the arugula leaf to enable transformation of sub-cuticle cell types, such as mesophyll cells. Consequently, we tested the transformation of mature *Nicotiana benthamiana* plant leaves with the gene gun and obtained GFP expression in mesophyll cells, most likely due to the fact that, as a model laboratory plant, *Nicotiana benthamiana* has a thin and easy-to-penetrate leaf structure[29] (**Supplementary Fig. 4**).

Spatial distribution analysis of CNT nanocarriers inside a plant leaf

After infiltration into the plant leaves, DNA-CNTs diffuse in the extracellular matrix while simultaneously internalizing into the plant cells. Consequently, there is a point where no nanocarrier is left in the extracellular matrix due to the consumption by cells proximal to the DNA-CNT infiltration area. We analyzed and modeled the spatial distribution of nanocarriers inside the leaf with a diffusion-reaction equation in which we implement a first order elementary reaction with a constant rate constant for metabolic consumption of nanocarriers (see Supplementary Information). The model predicts an exponential decay in the concentration of nanocarriers with respect to distance from the infiltration area. To fit this mathematical model to our experimental results, we analyzed the lateral profile of leaf GFP fluorescence expression obtained through confocal imaging as a proxy for nanocarrier diffusivity, and obtain good agreement between our diffusion-reaction model and GFP fluorescence localization (R^2 = 0.996, **Supplementary Fig. 5**). Additionally, near-infrared fluorescence images of DNA-SWCNT diffusion and lateral spatial distribution in leaves match our observed GFP expression profiles with confocal microscopy (**Supplementary Fig. 6**).

DNA delivery into isolated protoplasts with carbon nanotube scaffolds

We further investigated the ability of CNT nanocarriers to deliver plasmid DNA and trigger functional gene expression in a different plant system – isolated protoplasts, which are cultured plant cells without cell walls. Currently, protoplasts are used to increase the throughput of plant genetic screens and for synthesis of recombinant proteins, thus needing a facile, passive, high efficiency, and species-independent transformation platform[30]. For this purpose, intact and healthy protoplasts were extracted from arugula leaves through enzymatic cell wall degradation (see Methods, **Fig. 4a**) with high efficiency and high yield (10^7 total protoplast / 10 leaves). The

isolated protoplast solution was incubated with plasmid DNA-CNTs, and subsequently imaged with fluorescence microscopy to gauge GFP expression. Additional to the plasmid used in leaf studies (35S-GFP, **Supplementary Fig. 7**)**,** for protoplast experiments we also used a plasmid that encodes a nuclear localization signal (UBQ10-GFP, **Supplementary Fig. 7**), which transports the expressed GFP from the cytosol into the nucleus. Protoplasts incubated with both types of DNA-CNTs show strong GFP expression correctly localized in cells, whereas protoplasts incubated with free plasmids without CNTs do not show GFP expression (**Fig. 4b**). Our protoplast transformation efficiencies are 76% and 86% with UBQ10-CNTs and 35S-CNTs, respectively (**Fig. 4c** and **Supplementary Fig. 8**). Our prior work on CNT nanoparticle internalization into extracted plant plastids suggests nanoparticle internalization through the lipid bilayer occurs within seconds of CNT exposure[16]. Thus, our CNT-based plasmid DNA delivery platform enables rapid and passive delivery of DNA into protoplasts and transgene expression with high efficiency and no observable adverse effects to protoplast viability.

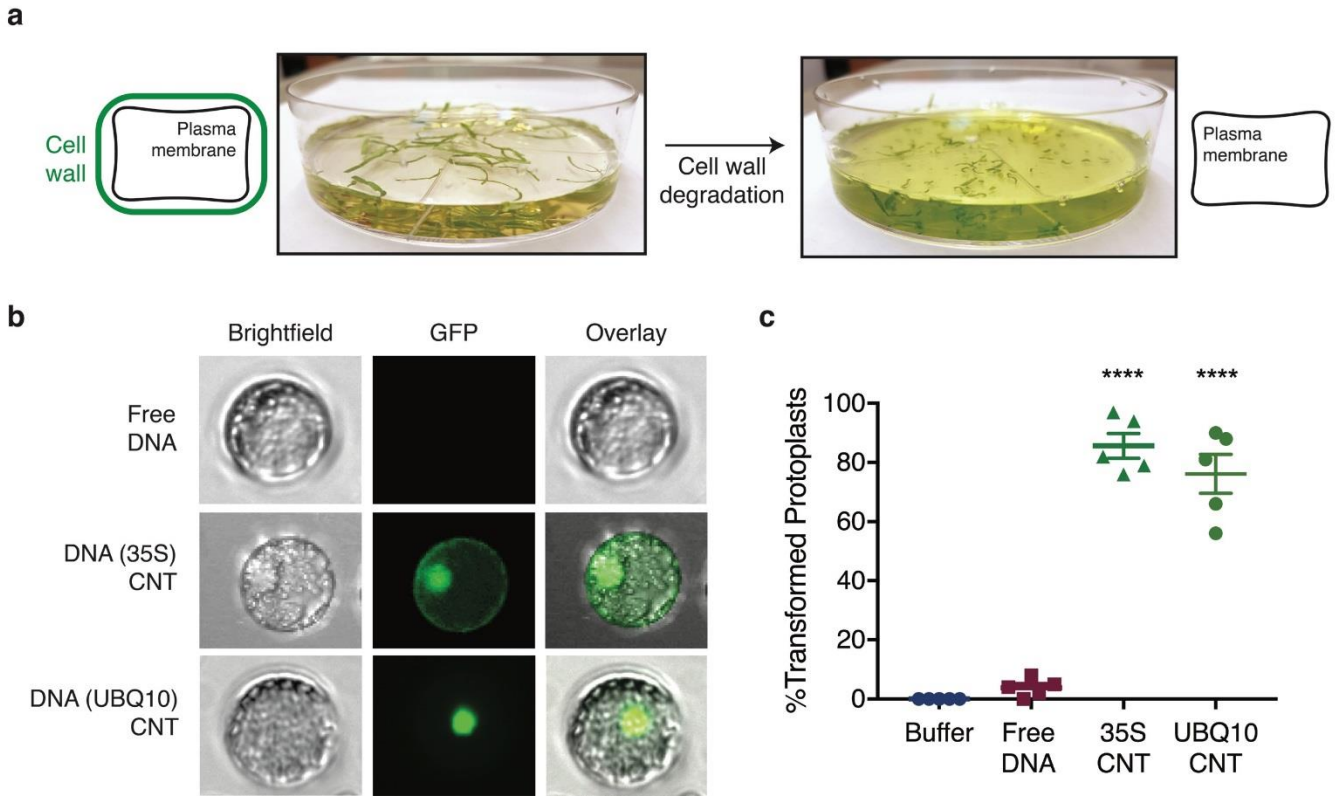

Figure 4. DNA delivery into isolated protoplasts with CNTs and subsequent GFP expression. (**a**) Intact and healthy protoplasts are extracted from arugula leaves through enzymatic cell wall degradation with high efficiency and high yield (10^7 total protoplast / 10 leaves). (**b**) Protoplasts incubated with 35S and UBQ10 DNA-CNTs show strong GFP expression correctly localized in cells. Protoplasts incubated with free DNA without CNT nanocarriers do not show GFP expression. Protoplast diameters are ~20 µm. (**c**) Percentage of the total isolated protoplasts transformed with 35S-CNTs is 86% and with UBQ10-CNT is 76% after a 24-hour incubation period. ****P < 0.0001 in one-way ANOVA. Error bars indicate s.e.m. (n = 5).

Carbon nanotube-guided siRNA gene silencing in mature plants

We next demonstrate the applicability of our CNT-mediated delivery tool in plants with another broadly-utilized functional cargo – siRNA, which is a short RNA duplex that acts within the RNA interference (RNAi) pathway for sequence-specific inhibition of gene expression at the mRNA transcript level[31]. As with plasmid DNA, delivery of siRNA has been optimized for most mammalian and bacterial cell culture applications, but remains a significant challenge for mature plants[32]. For this study, we silence a gene in transgenic *Nicotiana benthamiana*, which strongly expresses GFP in all cells due to GFP transgene integration in the nuclear genome. To silence this constitutively-expressed GFP gene, we designed a 21-bp siRNA sequence that is specific to the GFP mRNA[33] (**Fig. 5a**). Loading of siRNA on CNTs is accomplished by probe-tip sonication of each siRNA single-strand (sense and antisense) with SWCNTs (see Methods and **Fig. 5a**). The adsorption of RNA on SWCNTs was confirmed through the emergence of characteristic peaks in the SWCNT near-infrared fluorescence emission spectra for both siRNA sense and antisense suspensions (**Supplementary Fig. 9**). The mixture of siRNA sense and antisense loaded CNTs was infiltrated into the leaves of mature transgenic *Nicotiana benthamiana* plants. Post-infiltration, we predict that RNA-CNTs traverse the plant cell wall and membrane, and reach the cytosol. In the plant cell cytosol, the complementary siRNA strands hybridize to each other, desorb from the CNT surface, and induce GFP gene silencing through the RNAi pathway (**Fig. 5a**). Cytosolic hybridization and desorption claims are supported by our thermodynamics analysis that considers the energetics of hydrogen bonding and π-π stacking interactions, which found out to favor siRNA hybridization and desorption over adsorption on CNTs only in the intracellular environment (see Supplementary Information and **Supplementary Fig. 9**).

Nicotiana benthamiana leaves were imaged via confocal microscopy to monitor GFP silencing at the protein level. Untreated leaves show strong GFP expression, as expected, due to the constitutive expression of GFP in the transgenic plant. Conversely, leaves infiltrated with siRNA-CNTs show reduced GFP fluorescence via confocal microscopy (**Supplementary Fig. 10**), suggesting effective siRNA-CNT mediated gene silencing. Moreover, Western blot analysis reveals 43% reduction in GFP extracted from siRNA-CNT treated leaves compared to the leaves treated with non-targeting RNA loaded CNTs (NT-CNT) at two days post-infiltration (**Fig. 5b**). To corroborate our confocal imaging and Western blot results, we performed qPCR analysis of the siRNA-CNT infiltrated plant leaf tissue to quantify silencing at the mRNA transcript level. No significant gene silencing is observed in the non-treated leaf, nor in leaves infiltrated with non-

targeting RNA-CNTs, nor in leaves infiltrated with free GFP-targeting siRNA (**Fig. 5c**), whereby 95% reduction in GFP mRNA is observed when GFP-targeting siRNA is delivered via CNT scaffolding. It is likely that CNT scaffolding improves internalization of siRNA and also protects siRNA from degradation inside the cells. 7-days following the introduction of siRNA-CNTs, GFP expression as measured by qPCR returns to baseline levels as observed in non-treated leaves (**Fig. 5d**). A separate trial shows we are able to recover 71% GFP silencing at Day 7, as measured by qPCR, through the re-infiltration of the siRNA-CNT suspension at Day 5 (**Supplementary Fig. 10**).

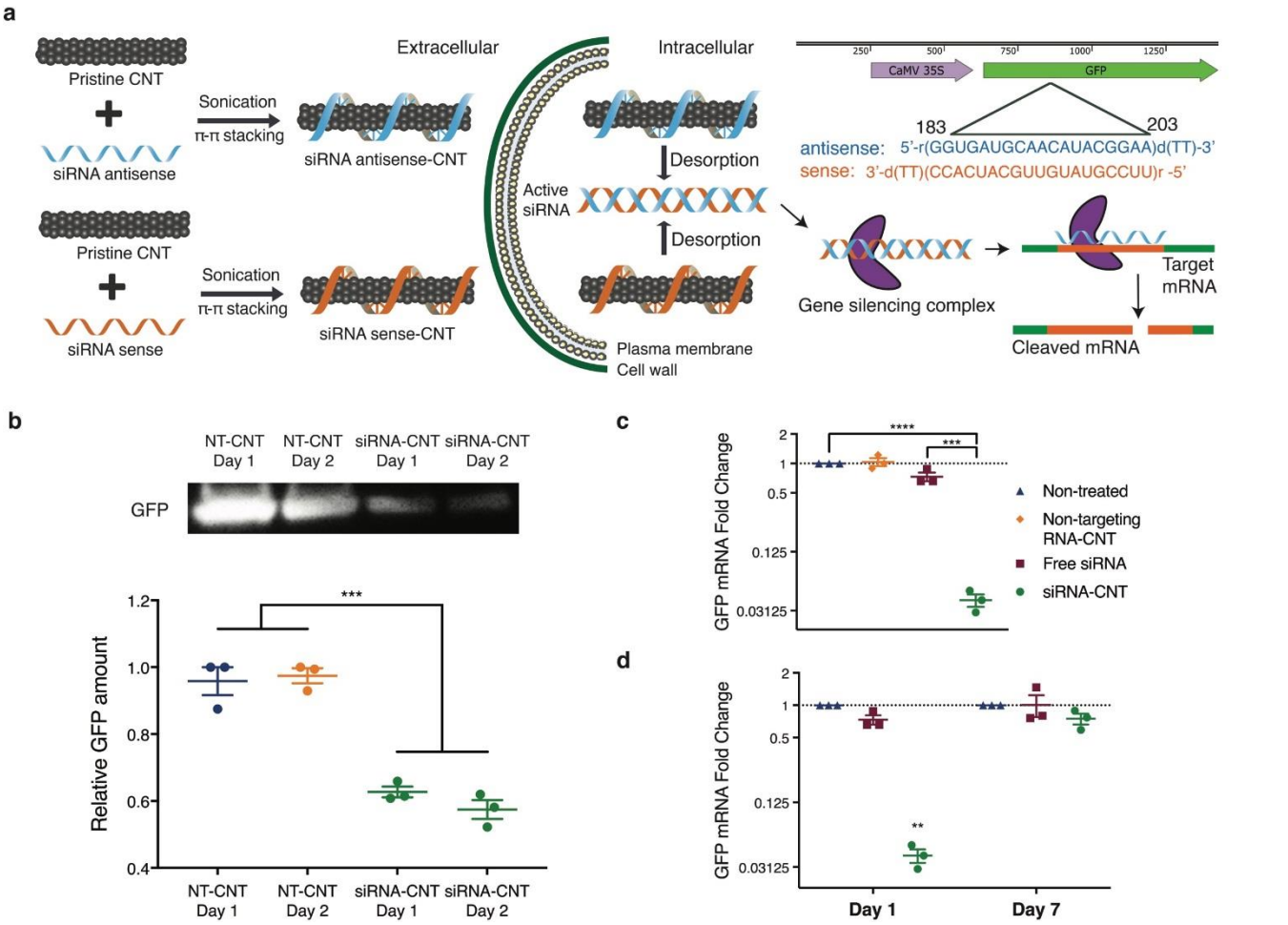

Figure 5. CNT-guided siRNA gene silencing in mature plants. (**a**) Loading of siRNA on CNTs is accomplished by probe-tip sonication of siRNA sense and antisense sequences with CNTs. Post-infiltration, RNA-CNTs traverse the plant cell wall and membrane, and reach the cytosol. The complementary siRNA strands hybridize to each other and desorb from the CNT surface. The desorbed siRNA activates the gene silencing complex, and acts as a template for complementary mRNA transcript recognition and cleavage. (**b**) A representative Western blot showing GFP extracted from non-targeting RNA-CNTs (NT-CNT) and siRNA-CNT treated leaves at one and two days post-infiltration. GFP Western blot band intensity analysis shows an average of 43% GFP reduction in siRNA-CNT infiltrated leaves compared to the NT-CNT infiltrated leaves at two-day post-infiltration. ***P = 0.0001 in one-way ANOVA. Error bars indicate s.e.m. (n = 3). (**c**) qPCR results show no significant gene silencing in the non-treated leaf, nor in leaves infiltrated with NT-CNT, nor with free GFP-targeting siRNA, whereby 95% gene silencing efficiency is observed when GFP-targeting siRNA is delivered via CNT scaffolding. ***P = 0.0002 and ****P < 0.0001 in one-way ANOVA. Error bars indicate s.e.m. (n = 3). (**d**) GFP expression nearly returns to its initial value 7-days

post-infiltration with siRNA-CNT, suggesting transient gene silencing. ***P* = 0.0014 in two-way ANOVA. Error bars indicate s.e.m. (n = 3).

Analysis of CNT toxicity to plant leaves

qPCR analysis, through normalization with the plant reference gene elongation factor 1 (EF1) expression[34], confirms that the observed decrease in GFP expression is triggered by CNT-mediated siRNA delivery, and it is not due to infiltration-mediated damage of the leaf tissue. To further confirm this claim, we undertook plant toxicity analyses. Specifically, we performed qPCR analysis of respiratory burst oxidase homolog B (NbrbohB) upregulation (**Supplementary Fig. 11**), a known stress gene in *Nicotiana benthamiana* plants[35]. Quantification of NbrbohB expression shows that CNT-treated areas in leaves do not upregulate NbrbohB compared to adjacent areas within the same leaves treated only with buffer. Additionally, quantum yield measurements of photosystem II[36] show that CNT-infiltrated areas in the *benthamiana* leaves have similar photosynthesis quantum yields as control areas within the same leaves without CNT infiltration. Positive controls to induce plant stress for both NbrbohB qPCR and photosystem II quantum yield measurements show clear upregulation of NbrbohB and significant decrease in photosystem II quantum yield in *Nicotiana benthamiana* (**Supplementary Fig. 11**). Our analysis concludes that the CNT-based delivery platform does not induce any toxicity to mature plants at the concentrations used in this study.

DISCUSSION

Genetic engineering of plants may address the crucial challenge of cultivating sufficient food and natural product therapeutics for an increasing global population living under changing climatic conditions. Despite advances in genetic engineering across many biological species, the transport of biomolecules into plant cells and nuclei remain the primary limitation for broad-scale implementation and high-throughput testing of genetic engineering tools, particularly for mature plants with walled cells. We thus present a nanomaterial-based delivery platform that permits diverse conjugation chemistries to achieve DNA delivery for transient transformations in both model and crop plants, and in both dicot and monocot plants, with high efficiency and no toxicity. In this study, we show the development and optimization of dialysis and electrostatic grafting methods for loading biomolecules onto high aspect ratio CNTs. We confirm the feasibility and test the efficacy of this platform by delivering reporter DNA constructs into mature arugula and wheat leaves, and protoplasts, and obtain strong transient expression of a functional transgenic protein. The value of the developed platform is also demonstrated through high

transient gene silencing obtained via CNT-mediated siRNA delivery. The nanomaterial-based transient plant transformation technology developed herein is beneficial for plant biotechnology applications where gene expression without transgene integration is desired, and is amenable to multiplexing whereby multiple gene vectors are to be delivered and tested rapidly and in parallel[37]. This technology may aid high-throughput screening of mature plants to rapidly identify genotypes that result in desired phenotypes, mapping and optimization of plant biosynthetic pathways, and maximization of plant-mediated natural product synthesis, most of which currently rely on agrobacterial transformation[38]. CNT-mediated biomolecule delivery to plants is easy and fast, transient, species-independent, and scalable, enabling its broad-scale adoption in plant biotechnology.

Additionally, global regulatory oversight for genetically-modified organisms (GMOs) motivate the future development of transient and/or DNA-free plant biotechnologies in which the gene expression is transient and foreign DNA is not integrated into the plant genome. However, the most commonly used tool today for plant genetic transformations – agrobacterium technology – is unable to perform DNA-free editing, yields random DNA integration, and has highly limited plant host range. The alternative technology, biolistic DNA delivery, may enable DNA-free editing through the delivery of ribonucleoproteins (RNPs), however, is typically limited to undifferentiated plant tissue (such as calli and embryos), which requires arduous regeneration and tissue culture processes. Thus, research in developing plant transformation biotechnologies commensurate with rapidly changing regulatory oversight of genetically modified plants is warranted.

References

1. Daniell, H., Datta, R., Varma, S., Gray, S. & Lee, S.-B. Containment of herbicide resistance through genetic engineering of the chloroplast genome. *Nat Biotech* **16**, 345-348 (1998).
2. Liu, Y. *et al.* A gene cluster encoding lectin receptor kinases confers broad-spectrum and durable insect resistance in rice. *Nat Biotech* **33**, 301-305, doi:10.1038/nbt.3069 (2015).
3. Li, T., Liu, B., Spalding, M. H., Weeks, D. P. & Yang, B. High-efficiency TALEN-based gene editing produces disease-resistant rice. *Nat Biotech* **30**, 390-392, doi:10.1038/nbt.2199 (2012).
4. Zhang, G. *et al.* Overexpression of the soybean GmERF3 gene, an AP2/ERF type transcription factor for increased tolerances to salt, drought, and diseases in transgenic tobacco. *Journal of Experimental Botany* **60**, 3781-3796, doi:10.1093/jxb/erp214 (2009).
5. Chen, Q. & Lai, H. Gene delivery into plant cells for recombinant protein production. *Biomed Res Int* **2015**, 932161, doi:10.1155/2015/932161 (2015).
6. Himmel, M. E. *et al.* Biomass Recalcitrance: Engineering Plants and Enzymes for Biofuels Production. *Science* **315**, 804 (2007).
7. Tufekcioglu, A., Raich, J., Isenhart, T. & Schultz, R. Biomass, carbon and nitrogen dynamics of multi-species riparian buffers within an agricultural watershed in Iowa, USA. *Agroforestry Systems* **57**, 187-198 (2003).
8. Altpeter, F. *et al.* Advancing Crop Transformation in the Era of Genome Editing. *Plant Cell* **28**, 1510-1520, doi:10.1105/tpc.16.00196 (2016).
9. Herrera-Estrella, L., Depicker, A., Van Montagu, M. & Schell, J. Expression of chimaeric genes transferred into plant cells using a Ti-plasmid-derived vector. *Nature* **303**, 209-213 (1983).
10. Baltes, N. J., Gil-Humanes, J. & Voytas, D. F. Genome Engineering and Agriculture: Opportunities and Challenges. *Progress in Molecular Biology and Translational Science* (2017).
11. Klein, T. M., Wolf, E., Wu, R. & Sanford, J. High-velocity microprojectiles for delivering nucleic acids into living cells. *Nature* **327**, 70-73 (1987).
12. Russell, J. A., Roy, M. K. & Sanford, J. C. Physical trauma and tungsten toxicity reduce the efficiency of biolistic transformation. *Plant Physiology* **98**, 1050-1056 (1992).
13. Song, S., Hao, Y., Yang, X., Patra, P. & Chen, J. Using gold nanoparticles as delivery vehicles for targeted delivery of chemotherapy drug fludarabine phosphate to treat hematological cancers. *Journal of nanoscience and nanotechnology* **16**, 2582-2586 (2016).
14. Mizrachi, A. *et al.* Tumour-specific PI3K inhibition via nanoparticle-targeted delivery in head and neck squamous cell carcinoma. *Nature Communications* **8**, 14292 (2017).
15. Demirer, G. S. & Landry, M. P. Delivering Genes to Plants. *CHEMICAL ENGINEERING PROGRESS* **113**, 40-45 (2017).
16. Wong, M. H. *et al.* Lipid exchange envelope penetration (LEEP) of nanoparticles for plant engineering: A universal localization mechanism. *Nano letters* **16**, 1161-1172 (2016).
17. Giraldo, J. P. *et al.* Plant nanobionics approach to augment photosynthesis and biochemical sensing. *Nature materials* **13**, 400-408 (2014).
18. Wu, Y., Phillips, J. A., Liu, H., Yang, R. & Tan, W. Carbon nanotubes protect DNA strands during cellular delivery. *ACS nano* **2**, 2023-2028 (2008).
19. Zheng, M. *et al.* DNA-assisted dispersion and separation of carbon nanotubes. *Nature materials* **2**, 338 (2003).

20. Wang, H. *et al.* High-yield sorting of small-diameter carbon nanotubes for solar cells and transistors. *ACS nano* **8**, 2609-2617 (2014).
21. Liu, Q. *et al.* Carbon nanotubes as molecular transporters for walled plant cells. *Nano letters* **9**, 1007-1010 (2009).
22. Serag, M. F. *et al.* Trafficking and subcellular localization of multiwalled carbon nanotubes in plant cells. *ACS nano* **5**, 493-499 (2010).
23. Wong, M. H. *et al.* Nitroaromatic detection and infrared communication from wild-type plants using plant nanobionics. *Nature materials* **16**, 264-272 (2017).
24. Choi, J. H. & Strano, M. S. Solvatochromism in single-walled carbon nanotubes. *Applied Physics Letters* **90**, 223114 (2007).
25. Alidori, S. *et al.* Deploying RNA and DNA with functionalized carbon nanotubes. *The Journal of Physical Chemistry C* **117**, 5982-5992 (2013).
26. Boehr, D. D., Farley, A. R., Wright, G. D. & Cox, J. R. Analysis of the π-π stacking interactions between the aminoglycoside antibiotic kinase APH (3′)-IIIa and its nucleotide ligands. *Chemistry & biology* **9**, 1209-1217 (2002).
27. Volkov, A. & Coppens, P. Calculation of electrostatic interaction energies in molecular dimers from atomic multipole moments obtained by different methods of electron density partitioning. *Journal of Computational Chemistry* **25**, 921-934, doi:10.1002/jcc.20023 (2004).
28. Tinland, B. The integration of T-DNA into plant genomes. *Trends in Plant Science* **1**, 178-184, doi:https://doi.org/10.1016/1360-1385(96)10020-0 (1996).
29. Díaz T, P., Bernal G, A. & López C, C. Transient GUS gene expression in cassava (Manihot esculenta Crantz) using Agrobacterium tumefaciens leaf infiltration. *Revista MVZ Córdoba* **19**, 4338-4349 (2014).
30. Schaumberg, K. A. *et al.* Quantitative characterization of genetic parts and circuits for plant synthetic biology. *Nature methods* **13**, 94 (2016).
31. Hannon, G. J. RNA interference. *Nature* **418**, 244-251 (2002).
32. Wittrup, A. & Lieberman, J. Knocking down disease: a progress report on siRNA therapeutics. *Nature reviews. Genetics* **16**, 543 (2015).
33. Tang, W. *et al.* Post-transcriptional gene silencing induced by short interfering RNAs in cultured transgenic plant cells. *Genomics, proteomics & bioinformatics* **2**, 97-108 (2004).
34. Schmidt, G. W. & Delaney, S. K. Stable internal reference genes for normalization of real-time RT-PCR in tobacco (Nicotiana tabacum) during development and abiotic stress. *Molecular Genetics and Genomics* **283**, 233-241, doi:10.1007/s00438-010-0511-1 (2010).
35. Yoshioka, H. *et al.* Nicotiana benthamiana gp91phox homologs NbrbohA and NbrbohB participate in H2O2 accumulation and resistance to Phytophthora infestans. *The Plant Cell* **15**, 706-718 (2003).
36. Van Kooten, O. & Snel, J. F. The use of chlorophyll fluorescence nomenclature in plant stress physiology. *Photosynthesis research* **25**, 147-150 (1990).
37. Sullivan, A. M. *et al.* Mapping and dynamics of regulatory DNA and transcription factor networks in A. thaliana. *Cell reports* **8**, 2015-2030 (2014).
38. Lau, W. & Sattely, E. S. Six enzymes from mayapple that complete the biosynthetic pathway to the etoposide aglycone. *Science* **349**, 1224-1228 (2015).

ACKNOWLEDGMENTS

We acknowledge support of a Burroughs Wellcome Fund Career Award at the Scientific Interface (CASI), the Simons Foundation, a Stanley Fahn PDF Junior Faculty Grant with Award # PF-JFA-1760, a Beckman Foundation Young Investigator Award, and a FFAR New Innovator Award. M.P.L. is a Chan Zuckerberg Biohub investigator. G.S.D. is supported by a Schlumberger Foundation Faculty for the Future Fellowship. L.C. is supported by National Defense Science and Engineering Graduate (NDSEG) Fellowship and by the LAM Foundation. The authors wish to thank Dr. Myeong-Je Cho for assisting with gene gun experiments, Christopher Gee for assisting with the Imaging-PAM Maxi fluorimeter, Dr. Alex Schultink and Arturo Ortega for helpful discussions, and Dr. Christopher Jakobson and Dr. Danielle Tullman-Ercek for generously sharing their lab resources. We acknowledge the support of the UC Berkeley Molecular Imaging Center, the QB3 Shared Stem Cell Facility, and the Innovative Genomics Institute (IGI).

AUTHOR CONTRIBUTIONS

G.S.D. and M.P.L. conceived of the project, designed the study, and wrote the manuscript. G.S.D. and R.C. performed experiments and data analysis. J.L.M performed agrobacterium, gene gun and wheat transformation experiments. H.Z. and L.C. performed AFM imaging data analysis. All authors have edited and commented on the manuscript, and have given their approval of the final version.

COMPETING FINANCIAL INTERESTS

The authors declare no competing financial interests.

ONLINE METHODS

Procurement and preparation of chemicals and nanomaterials. Super purified HiPCO SWCNTs (Lot # HS28-037) were purchased from NanoIntegris, MWCNTs (Lot # R0112) were purchased from NanoLab, and both CNT samples were extensively purified before use[1]. Carboxylic acid functionalized SWCNTs (Lot # MKBX0303V) and MWCNTs (Lot # BCBR9248V) were purchased from Sigma-Aldrich. GFP-encoding dicot plasmids (35S-GFP-NOS and UBQ10-GFP-NOS) were obtained from the Sheen Lab, Harvard Medical School[2]. GFP-encoding monocot plasmid (osACTIN-GFP-NOS) was obtained from the Staskawicz Lab, UC Berkeley. 20K MWCO dialysis cassettes were purchased from Thermo Scientific. The following chemicals were purchased from Sigma-Aldrich: stains-all dye (95%), sodium dodecyl sulfate (molecular biology grade), sodium chloride, MES hydrate, D-mannitol, calcium chloride dihydrate (suitable for plant cell culture), potassium chloride, magnesium chloride hexahydrate, bovine serum albumin (heat shock fraction), polyethylene glycol (4 K), and polyethylenimine (branched, 25 K). Cellulase R10 and macerozyme R10 enzymes were purchased from Grainger. Single stranded RNA and DNA polymers were purchased from IDT and dissolved in 0.1M NaCl before use. UltraPure DNase/RNase-free distilled water from Invitrogen was used for qPCR experiments, and EMD Millipore Milli-Q water was used for all other experiments.

Plant growth. Italian arugula *(Eruca sativa)* seeds purchased from Renee's Garden were germinated in SunGro Sunshine LC1 Grower soil mix by planting the seeds half an inch deep into the soil of a standard propagation liner tray (Nursery Supplies). The germinated plants were then moved to a Hydrofarm LED growth chamber (12h light at ~22˚C / 12h dark at 18˚C). Plants were allowed to mature to 3-4 weeks of age within the chamber before experimental use. Transgenic mGFP5 *Nicotiana benthamiana* seeds obtained from the Staskawicz Lab, UC Berkeley, were germinated and grown in SunGro Sunshine LC1 Grower soil mix for four weeks before experimental use. Spring wheat (*Triticum aestivum L.*, cv. Fielder) were grown in Supersoil (Rod McClellan Co., South San Francisco, CA, USA) in a Conviron growth chamber with 60% relative humidity, 18-hour light at 24°C: 8-hour dark at 18°C cycle, and 3-4-week-old plants were used for experiments.

SDS-CNT, siRNA-CNT, and ssDNA-CNT preparation. 1 mg/mL HiPCO SWCNTs were added to 3 mL 2 wt% SDS in water and bath sonicated for 10 min, followed by probe-tip sonication with a 6-mm sonicator tip at 40% amplitude (~12W) for 1h in an ice bath. The resulting solution rested at room temperature for 30 minutes before centrifugation at 16,100g for 1 h to remove unsuspended SWCNT aggregates and metal catalyst precursor. The concentration of SDS-SWCNTs was measured by recording the SWCNT absorption spectrum with a UV-Vis-nIR spectrometer and calculating the SWCNT concentration in mg/liter (absorbance at 632 nm/extinction coefficient of 0.036). The same suspension protocol applies for MWCNTs, but, their concentration was measured using a standard curve as obtained by Yang *et al.* [3].

The sequences of siRNA that were utilized for siRNA gene silencing experiments are: sense strand: 5'-r(GGUGAUGCAACAUACGGAA)d(TT)-3' and antisense strand: 5'-r(UUCCGUAUGUUGCAUCACC)d(TT)-3'.
The sequences of the non-targeting RNA strands are sense: 5'-r(UAAGGCUAUGAAGAGAUAC)d(TT)-3' and antisense: 5'-r(GUAUCUCUUCAUAGCCUUA)d(TT)-3'.

siRNA and non-targeting RNA were loaded on SWCNTs as single-stranded polymers through probe-tip sonication as previously described[4]. Briefly, the sense strand of siRNA was dissolved at a concentration of 100 mg/mL in 0.1 M NaCl. 20 µL of this RNA solution was aliquoted into 980 µL 0.1 M NaCl and 1 mg HiPCO SWCNTs was added. The mixture was bath sonicated for 10 min, followed by probe-tip sonication with a 3-mm tip at 50% amplitude (~7W) for 30 min in an ice bath. The resulting solution rested at room temperature for 30 minutes before centrifugation at 16,100g for 1 h to remove unsuspended SWCNT aggregates and metal catalyst precursor. The same protocol was followed for the antisense strand of siRNA and non-targeting RNA strands. Unbound (free) RNA was removed via spin-filtering (Amicon, 100 K) and the concentration of RNA-SWCNTs was determined by measuring the SWCNT absorbance at 632 nm. For toxicity assays, SWCNTs were suspended in single-stranded DNA (ssDNA) polymers with the sequence $(AT)_{15}$. Preparation of ssDNA-SWCNTs followed the same protocol as for RNA-loaded SWCNTs, described above.

Linear DNA vector preparation from plasmid DNA. The promoter, GFP gene, and terminator regions of the 35S-GFP-NOS plasmid (obtained from the Sheen Lab, Harvard Medical School) were amplified with PCR over 35 cycles, with the following modified M13 forward and M13 reverse primers: 5'-GTAAAACGACGGCCAGT-3' and 5'-AGCGGATAACAATTTCACACAGG-3', respectively. Following PCR, pure DNA vector was obtained by using a PureLink PCR purification kit (Invitrogen) to eliminate primers, unreacted nucleotides, and enzymes. To check the

amplification quality, the resulting amplicon was sent for Sanger sequencing, and was also run with agarose gel electrophoresis (see **Supplementary Fig. 7** for plasmid maps and linearization results).

Direct adsorption of DNA onto CNTs via dialysis. SDS-CNT solution containing 1 µg of CNTs, and 10 µg of free plasmid DNA were placed into an accurately-pore-sized dialysis cartridge (20 K, 0.5 mL), that allowed the exit of SDS monomers that desorbed from the CNT surface, while free plasmid DNA suspended the CNTs which remained inside the dialysis cartridge. If necessary due to volume considerations, 2 wt% SDS was used to fill the additional volume of dialysis cartridge to ensure there was no free air space in the cartridge. After 4 days of dialysis with continuous stirring at room temperature and changing the dialysis buffer (0.1M NaCl) daily, we obtained a stable suspension of plasmid DNA conjugated CNTs. The preparation protocol was same for both plasmids and linearized DNA vectors, and for both types of CNTs (SW- and MWCNTs). The near-infrared (nIR) fluorescence spectra of dialysis suspended CNTs are obtained through a nIR fluorescence microscopy using 721nm laser excitation and an inverted microscope outfitted with an InGaAs sensor array for imaging[4].

Control studies for dialysis. A control cartridge consisting of an SDS-CNT solution that contains 1 µg of CNTs in 2 wt% SDS, but lacking DNA, was dialyzed in parallel under the same conditions to ensure that CNTs did not suspend in solution in the absence of plasmid DNA, confirming plasmid DNA adsorption to CNTs in the main sample. Stains-all dye, which changes color in the presence of SDS, is used to determine %SDS in the dialysis cartridge. A standard curve with the range of 0-0.016 %SDS is created at the absorbance wavelength 453 nm. Five dialysis formulations, as described above, are prepared and they are stopped at different time points along the duration of dialysis (Day 0, 1, 2, 3 and 4). 10 µL of dialysis solution is mixed with 1 mL 0.1% stains-all (w:v in formamide), and absorbance at 453 nm is measured. By using the standard curve, precise SDS% in the cartridge is calculated at each day point.

Electrostatic grafting of DNA onto CNTs. Chemical modification of CNTs to carry positive charge is described elsewhere[5] and applied here with some modifications. A mixture of 100 mg of carboxylated CNTs suspended in water (1 mg/mL) and 1 g of PEI solution was bath sonicated for several minutes, and subsequently heated at 82 °C with stirring for 16 h (the reaction can be scaled up or down as desired by keeping the PEI to CNT mass ratio constant). The reaction mixture was subsequently cooled to room temperature and filtered with a 0.4 µm and 1 µm Whatman Nucleopore membrane to filter SWCNTs and MWCNTs, respectively. The filtered product was washed vigorously with water 10 times to remove unreacted PEI from the reaction mixture, then dried and collected. 3 mg of dried product (PEI-CNT) was subsequently suspended in 3 mL water by probe-tip sonication with a 6-mm tip at 40% amplitude (~12 W) for 1 h in an ice bath. The resulting solution was rested at room temperature for 30 minutes before centrifugation at 16,100g for 1 h to remove unsuspended CNT aggregates. The PEI-CNT solution containing 1 µg of CNTs was added into 0.2 µg of DNA dropwise, pipetted in and out 10 times, and incubated at room temperature for 30 minutes so that negatively charged DNA adsorbed on PEI-CNTs (DNA incubation can be scaled up or down as well by keeping the DNA to PEI-CNT mass ratio constant).

Infiltration of leaves with CNTs. Healthy and fully-developed leaves from *Eruca sativa* (arugula) plants (3-4 weeks old) and *Nicotiana benthamiana* plants (4 weeks old) were selected for experiments. A small puncture on the abaxial

surface of the *Eruca sativa* leaf lamina was introduced with a pipette tip, and 100 µL of the plasmid DNA-CNT solution was infiltrated from the hole with a 1 mL needleless syringe by applying a gentle pressure, with caution not to damage the leaf. For *Nicotiana benthamiana* infiltration, a tiny puncture on the abaxial surface of the leaf lamina was introduced with a sharp razor, and 100 µL of siRNA-CNT solution was infiltrated through the puncture with a 1 mL needleless syringe by applying a gentle pressure. After infiltration, leaves were left in the plant growth chamber (for arugula) and in plant pots (for *benthamiana*) to allow for gene expression and silencing, and imaged after 72 and 24 h, respectively, prior to quantifying gene expression and silencing. For wheat leaf infiltrations, a sharp razor blade was used to produce a small puncture on the abaxial surface of 3-4-week-old plants, and 100 µL of the plasmid DNA-CNT solution was infiltrated with a 1 mL needless syringe. Plants were returned to growth chamber and imaged after 3 and 10 days-post-infiltration.

Quantitative fluorescence intensity analysis of GFP gene expression. Infiltrated *Eruca sativa* plant leaves were prepared for confocal imaging 72-hours post-infiltration with DNA-CNT by cutting a small leaf section of the infiltrated leaf tissue, and inserting the tissue section between a glass slide and cover slip of #1 thickness. 100 µL water was added between the glass slide and cover slip to keep the leaves hydrated during imaging. A Zeiss LSM 710 confocal microscope was used to image the plant tissue with 488 nm laser excitation and with a GFP filter cube. GFP gene expression images were obtained at 10x magnification. Confocal image data was analyzed to quantify GFP expression across samples. For each sample, 3 biological replicates (3 infiltrations into 3 different plants) were performed, and for each biological replicate, 15 technical replicates (15 non-overlapping confocal field of views from each leaf) were collected. Each field of view was analyzed with custom ImageJ analysis to quantify the GFP fluorescence intensity value for that field of view, and all 15 field of views were then averaged to obtain a mean fluorescence intensity value for that sample. The same protocol was repeated for all 3 biological replicates per sample, and averaged again for a final fluorescence intensity value, which correlates with the GFP expression produced by that sample.

***Agrobacterium* transient expression.** *Agrobacterium tumefaciens* strain GV3101 was used for genetic transformation of *N. benthamiana* and arugula leaves. To generate the agrobacterium-binary construct, the DNA fragment containing 35S-GFP-NOS were excised from the plasmid 35sC4PPDKsGFPTYG with the restriction enzymes XhoI and EcoRI and cloned into an entry cloned digested with the same restriction enzymes. The 35S-GFP-NOS entry clone was recombined into the agrobacterium destination vector pPZP201[6]. Agrobacterium suspensions (OD_{600} = 0.4) were infiltrated into *N. Benthamiana* and arugula leaves of 3-4-week-old plants using a 1-ml needleless syringe. Plants were returned to the growth chamber and imaged after 3 and 10 days-post-infiltration.

Biolistic delivery of plasmid DNA. *N. Benthamiana* and arugula seeds were sterilized in solution (20% bleach) for 30 minutes under gentle agitation, then washed three times with sterile water, plated on ½ Murashige and Skoog (MS) medium, stratified for 2 days at 4˚C before transferring to a 26˚C incubator with 16-hour light: 8-hour dark cycle for growth. 3-wk-old leaves were placed onto semi-solid pre-shooting media [4.43 g/L of MS basal medium

and vitamins (M519); 36.43 g/L of Mannitol; 36.43 g/L of Sorbitol; 0.30g of Casein enzymatic hydrolysate; 0.5 g/L of L-proline 2 mL/L of 2,4-D (1 mg/ml); pH 5.8; 3.5 g/L of Phytagel] in a small circle in the center of the plate to facilitate bombardment and incubated at 25°C for 4 hours in the dark. 35S-GFP DNA plasmid (35sC4PPDKsGFPTYG) was coated onto 0.6 µm (average diameter) gold nanoparticles (Bio-Rad): 1 mg of gold particles were mixed with 30 µl of DNA construct (0.17 µg/µl), 25 µl of 5.0 M $CaCl_2$ and 20 µl of 0.1 M spermidine and incubated on ice for 10 min. DNA-coated gold particles were collected at 10,000 rpm for 1 min, and the pellet was rinsed with 1 mL of absolute alcohol, resuspended in 85 µl ethanol, and then immediately loaded onto the center of a macrocarrier (5 µl each) and allowed to air dry. Biolistic bombardment was performed using a PDS1000/He particle bombardment system (Bio-Rad) with a target distance of 6.0 cm and a rupture pressure of 900 PSA. After bombardment, leaves were transferred to MS solid medium and imaged at 3 and 10 days-post-bombardment.

Quantitative Western blot experiments and data analysis. Infiltrated plant leaves were harvested after 48 h and grounded in liquid nitrogen to get dry frozen powders. The frozen powders were transferred to a tube with pre-prepared lysis buffer containing 10 mM Tris/HCl (pH 7.5), 150 mM NaCl, 1 mM EDTA, 0.1% NP-40, 5% glycerol, and 1% Cocktail. After lysis at 4℃ overnight, the tube was centrifuged at 10,000 rpm for 15 minutes and the supernatant containing whole proteins was collected to a new tube. After quantification of the total extracted proteins by Pierce 660 nm Protein Assay (Thermo, Prod# 22660), 0.5 µg of normalized total proteins from each sample were analyzed by 12% SDS–PAGE and blotted to PVDF membrane. The membrane was blocked for 1 hour using 7.5% BSA in PBST (PBS containing 0.1% Tween20) buffer and incubated overnight at 4°C with the primary GFP antibody as required (1:2000 dilution, Abcam, ab290). After extensive washing, the corresponding protein bands were probed with a goat anti-rabbit horseradish peroxidase-conjugated antibody (1:5000 dilution, Abcam, ab205718) for 30 min. The membrane was then developed by incubation with chemiluminescence (Amersham ECL prime kit) plus and imaged by ChemiDoc™ XRS+ System (BIORAD). The intensity of GFP bands were quantified with ImageJ software.

Protoplast isolation from *Eruca sativa* leaves. Protoplasts were isolated from arugula leaves as described by Yoo *et al.*[2] with some modifications. Briefly, thinly cut arugula leaf strips were immersed in 20 mL of enzyme solution (consisting of cellulase and macerozyme), vacuum infiltrated for an hour in the dark using a desiccator, and further incubated at 37˚C for 3 hours in the dark without stirring. Undigested leaf tissue was removed by filtration with a 75 µm nylon mesh, and the flow-through was centrifuged at 200 g for 3 min to pellet the protoplasts in a round bottom tube. Pelleted protoplasts were resuspended in 0.4 M mannitol solution (containing 15 mM $MgCl_2$ and 4 mM MES) with a pH of 5.7, which has similar osmolarity and pH to the protoplasts. Isolated protoplasts can be kept viable on ice for over 24 h; however, we used only freshly isolated protoplasts for all gene expression studies.

Protoplast transformation with DNA-CNTs. 100 µL (~$2x10^4$) of isolated protoplasts in mannitol solution were added to 10 µg CNT-plasmid DNA (250 ng/µL DNA concentration), or for the control sample only plasmid DNA (250

ng/μL DNA concentration) and mixed well by gently tapping the tube. The mixture was incubated at room temperature for 1 h, and subsequently centrifuged at 200g for 3 min to pellet protoplasts. Protoplasts were resuspended in 1 mL of 0.5 M mannitol solution (containing 4mM MES and 20 mM KCl at pH 5.7) in a non-culture treated 6 well-plate (Corning) for 24 hours in the dark. Protoplasts settled at the bottom of the well plate. Fluorescence microscopy was performed through the well-plate to image the protoplasts and to measure GFP expression for quantification of transformation efficiency.

Quantitative PCR (qPCR) experiments and data analysis. Two-step qPCR was performed to quantify GFP gene silencing in transgenic *Nicotiana benthamiana* plants with the following commercially-available kits: RNeasy plant mini kit (QIAGEN) for total RNA extraction from leaves, iScript cDNA synthesis kit (Bio-Rad) to reverse transcribe total RNA into cDNA, and PowerUp SYBR green master mix (Applied Biosystems) for qPCR. The target gene in our qPCR was mGFP5 (GFP transgene inserted into *Nicotiana benthamiana*), and EF1 (elongation factor 1) as our housekeeping (reference) gene. Primers for these genes were ordered from IDT. For mGFP5, primers used are: forward 5'- AGTGGAGAGGGTGAAGGTGATG-3' and reverse: 5'- GCATTGAACACCATAAGAGAAAGTAGTG-3'. Primers for EF1 are: forward: 5'-TGGTGTCCTCAAGCCTGGTATGGTTGT-3' and reverse: 5'-ACGCTTGAGATCCTTAACCGCAACATTCTT-3'.

Annealing temperature of 60˚C was used for qPCR, which we ran for 40 cycles.

qPCR data was analyzed by the ddCt method[7] to obtain the normalized GFP gene expression-fold change with respect to the EF1 housekeeping gene and control sample. For each sample, qPCR was performed as 3 technical replicates (3 reactions from the same isolated RNA batch), and the entire experiment consisting of independent infiltrations and RNA extractions from different plants was repeated 3 times (3 biological replicates).

Plant toxicity analysis. To test for plant stress and toxicity, the expression level of an oxidative stress gene (NbRbohB)[8] in *Nicotiana benthamiana* leaves was measured through qPCR with the following primers:

forward 5'-TTTCTCTGAGGTTTGCCAGCCACCACCTAA-3' and reverse 5'-GCCTTCATGTTGTTGACAATGTCTTTAACA-3'.

EF1 was again measured as a housekeeping gene with the same primer set as described above. An annealing temperature of 60˚C was used for qPCR, which we ran for 40 cycles, and the ddCt method was used to obtain the normalized NbRbohB expression-fold change with respect to the EF1 housekeeping gene and control sample.

As an additional toxicity assay, Fv/Fm ratios[9] of infiltrated *Nicotiana benthamiana* leaves were measured with an Imaging-PAM Maxi fluorimeter (Walz). A singular leaf was infiltrated from the abaxial surface, in three distinct locations within the same leaf, with buffer (0.1 M NaCl), 1 mg/L DNA-CNTs, or 10% SDS (positive control for toxicity). The fourth quadrant of the leaf was left unperturbed. The triply-infiltrated leaf was subsequently incubated for 24 hours without further perturbation. Subsequently, the infiltrated leaf was dark-adapted for 15-30 minutes and chlorophyll fluorescence-related parameters were measured with the Imaging-PAM Maxi fluorimeter to calculate the Fv/Fm ratio, commonly used to test for plant stress.

Statistics.

Zeta potential data. N = 5 replicates are zeta potential measurements of the same CNT suspension. Data are expressed as each measurement together with error bars indicating standard deviation. Significance is measured with one-way ANOVA with Tukey's multiple comparisons test. F = 371.1, COOH-CNT vs. PEI-CNT $P < 0.0001$ and PEI-CNT vs. DNA-PEI-CNT $P = 0.0086$.

AFM height data. N = 10 replicates are measurements of heights of different CNTs within the same CNT suspension. Data are expressed as each measurement together with error bars indicating standard deviation. Significance is measured with one-way ANOVA with Tukey's multiple comparisons test. F = 79.6, COOH-CNT vs. PEI-CNT $P = 0.02$ and PEI-CNT vs. DNA-PEI-CNT $P = 0.0002$.

Leaf GFP expression data. N = 3 replicates are independent experiments; 3 separate leaves infiltrated per sample and imaged. Each independent sample replicate contains 15 technical replicates (15 measurement from the same leaf). Confocal images reported in **Figure 2b** and **3a** are representative images chosen from the results obtained in 3 independent experiments for pDNA-PEI-SW sample. Data are expressed as each mean from the 3-independent experiments together with error bars indicating standard error of the mean. Significance is measured with one-way ANOVA with Tukey's multiple comparisons test. F = 22.33, Dialysis vs. electrostatic grafting samples $P < 0.0001$, and lDNA-PEI-SW vs. pDNA-PEI-SW $P = 0.001$. The same applies for **Figure 3b**, where N = 3 replicates are independent experiments and each independent sample replicate contains 15 technical replicates. Data are expressed as each mean from the 3-independent experiments together with error bars indicating standard error of the mean. Significance is measured with two-way ANOVA with Sidak's multiple comparisons test. DNA-CNT Day 3 vs. Day 10 $P = 0.0001$. For qPCR results reported in **Figure 3c,** N = 3 replicates are independent experiments; 3 separate leaves infiltrated per sample and measured with qPCR. Each sample in each independent experiment consisted of 3 technical replicates of the qPCR reaction. Data are expressed as each mean from the 3-independent experiments together with error bars indicating standard error of the mean. Significance is measured with two-way ANOVA with Sidak's multiple comparisons test. DNA-CNT Day 3 vs. Day 10 $P = 0.0003$.

Protoplast GFP expression data. N = 5 replicates are independent experiments; 5 separate protoplast solutions are incubated with samples and images with fluorescence microscopy. Images reported in **Figure 4b** are representative images chosen from the results obtained in 5 independent experiments. % transformation efficiency data are expressed as each mean from the 5-independent experiments together with error bars indicating standard error of the mean. Significance is measured with one-way ANOVA with Tukey's multiple comparisons test. F = 123.5, Buffer vs. DNA-CNT $P < 0.0001$, and Free DNA vs. DNA-CNT $P < 0.0001$.

siRNA silencing data. Western blot experiment has N = 3 replicates that are independent experiments, and **Figure 5b** denotes the results from a representative blot. Relative GFP amount data determined from the Western blot are expressed as mean from the 3-independent experiments together with error bars indicating standard error of the mean. Significance is measured with one-way ANOVA with Tukey's multiple comparisons test. F = 54.65, NT-CNT vs. siRNA-CNT $P = 0.0001$. For GFP mRNA fold change experiments in **Figure 5c**, N = 3 replicates are independent experiments, starting with RNA extraction from different leaves until the qPCR amplifications. Each qPCR reaction in 3 independent experiment is done in triplicate. GFP mRNA fold change data are expressed as each mean from the 3-independent experiments together with error bars indicating standard error of the mean. Significance is measured with one-way ANOVA with Tukey's multiple comparisons test. F = 57.64, Free siRNA vs. siRNA-CNT *P*

= 0.0002, and Non-treated vs. siRNA-CNT $P < 0.0001$. The same applies for **Figure 5d**, where N = 3 replicates are independent experiments. Data are expressed as each mean from the 3-independent experiments together with error bars indicating standard error of the mean. Significance is measured with two-way ANOVA with Sidak's multiple comparisons test. siRNA-CNT Day 1 vs. Day 7 $P = 0.0014$.

Data availability statement. Authors confirm that all relevant data are included in the paper and/or its supplementary information files.

References

1. Del Bonis-O'Donnell, J. T. *et al.* Engineering Molecular Recognition with Bio-mimetic Polymers on Single Walled Carbon Nanotubes. *JoVE (Journal of Visualized Experiments)*, e55030-e55030 (2017).
2. Yoo, S.-D., Cho, Y.-H. & Sheen, J. Arabidopsis mesophyll protoplasts: a versatile cell system for transient gene expression analysis. *Nature protocols* **2**, 1565 (2007).
3. Yang, M., Gao, Y., Li, H. & Adronov, A. Functionalization of multiwalled carbon nanotubes with polyamide 6 by anionic ring-opening polymerization. *Carbon* **45**, 2327-2333 (2007).
4. Beyene, A. G., Demirer, G. S. & Landry, M. P. Nanoparticle‐Templated Molecular Recognition Platforms for Detection of Biological Analytes. *Current protocols in chemical biology*, 197-223 (2016).
5. Ma, L. *et al.* Enhanced Li–S batteries using amine-functionalized carbon nanotubes in the cathode. *ACS nano* **10**, 1050-1059 (2015).
6. Hajdukiewicz, P., Svab, Z. & Maliga, P. The small, versatilepPZP family ofAgrobacterium binary vectors for plant transformation. *Plant Molecular Biology* **25**, 989-994, doi:10.1007/bf00014672 (1994).
7. Schmittgen, T. D. & Livak, K. J. Analyzing real-time PCR data by the comparative CT method. *Nature protocols* **3**, 1101 (2008).
8. Yoshioka, H. *et al.* Nicotiana benthamiana gp91phox homologs NbrbohA and NbrbohB participate in H2O2 accumulation and resistance to Phytophthora infestans. *The Plant Cell* **15**, 706-718 (2003).
9. Van Kooten, O. & Snel, J. F. The use of chlorophyll fluorescence nomenclature in plant stress physiology. *Photosynthesis research* **25**, 147-150 (1990).